

Synthesis and Crystal Structures of Cofacial Bisoctaethylchlorins as Structural Models for the Special Pair*

Werner W. Kalisch¹, Mathias O. Senge^{†1} and Karin Ruhlandt-Senge^{‡2}

¹ Institut für Organische Chemie, Freie Universität Berlin, Berlin, Germany and

² Department of Chemistry, Syracuse University, Syracuse, NY, USA

Received 15 September 1997; accepted 17 December 1997

ABSTRACT

Covalently linked bistetrapyrrole systems can be used to mimic structurally the arrangement of the two special pair bacteriochlorophylls in the bacterial photosynthetic reaction center. Such models require a cofacial arrangement of the two tetrapyrrole units with some overlap of the π systems and intramolecular stabilization by aggregation of the two macrocycles. Using the McMurry reaction for the coupling of metallo formyloctaethylchlorins, covalently linked cofacial bischlorins were prepared and characterized by spectroscopy and single crystal X-ray crystallography. Coupling of Ni(II)5-formyloctaethylchlorin yielded a (*Z*)-ethene-bridged bischlorin with cofacial orientation of the subunits stabilized by intramolecular π - π interactions that structurally resembles the situation found for the special pair in bacterial reaction centers. In addition, two different atropisomers of the respective (*E*)-ethene-bridged bischlorin were formed. Use of Cu(II)5-formyloctaethylchlorin yielded similar products, however a crystal structure showed a (*Z*)-ethene-bridged bischlorin without intramolecular stabilization *via* aggregation effects. The bischlorins are easily oxidized to mixed chlorin-porphyrin species.

INTRODUCTION

Since the elucidation of the crystal structures of the bacterial photosynthetic reaction center (1,2), there has been renewed interest in the synthesis of biomimetic model compounds for photosynthesis (3–5). While this work has evolved into the realm of functional models (6), a special challenge remains with the preparation of model compounds closely mimicking the cofactor arrangement found *in vivo*. Modeling of the intermediary and terminal cofactors of the electron transfer components can be achieved *via* synthesis of diad, triad or tetrad donor–acceptor complexes. Depending on the type

and the geometry of the bridging unit between the tetrapyrrole and quinone components complexes with linear extended or skewed geometry are possible (5). However, models for the special pair are more difficult to prepare, requiring the synthesis of (bacterio)chlorin dimers with a specific geometry—namely, a cofacial structure with parallel ring orientation and partial overlap of the two macrocycle π systems. Indeed, a wide variety of so-called “face-to-face” bistetrapyrroles have been prepared (3–11), including related bischlorophyll systems (12) (see Wasielewski (3,5) and Gust and Moore (4) for excellent reviews listing the pertinent literature). Nevertheless, interpretation of the photophysical properties of such compounds is often hampered by the absence of reliable structural data on the conformation, relative orientation and spatial arrangement of the subunits. Until recently, definite crystallographic data were available only for linear extended bischlorins (13) or cofacial bisporphyrins (see Senge *et al.* (15) and Scheidt and Lee (16) for a survey of the relevant literature) (13–16).

We have thus attempted the synthesis of structurally defined face-to-face bischlorins to provide access to model compounds for the special pair that then might be used for construction of larger multicomponent systems. Smith and coworkers recently found a convenient approach to cofacial bisporphyrins by utilization of the McMurry reaction (17,18) for the coupling of formylporphyrins (19). This method has enjoyed considerable success in Vogel’s porphycene syntheses (20) and upon application to the 5-formyl derivatives of simple metallo octaethylporphyrins (OEP)[§] like **2** or **3** gave the expected ethene-linked bisporphyrins. Surprisingly, the reaction products were not only the expected (*E*)-ethene-bridged bisporphyrins (*e.g.* **5** or **6**) but also the cofacial bisporphyrins linked by a (*Z*)-ethene bridge (*e.g.* **7** or **8**) (15,21). Formation of the (*Z*)-ethene-bridged bisporphyrins is presumably due to stabilization of the transition state by π - π aggregation of the subunits. The cofacial arrangement with almost planar macrocycles, stabilized by intramolecular π - π interactions evident in the crystal structures of **7** and **8**, closely resembles the situation found in the solid-state aggregates of monomeric metalloporphyrins (16,22). Like oth-

* Dedicated to Professor Horst Senger.

† To whom correspondence may be addressed at: Institut für Organische Chemie (WE02), Fachbereich Chemie, Freie Universität Berlin, Takustr. 3, D-14195 Berlin, Germany. Fax: 49-30-838-4248; e-mail: mosenge@chemie.fu-berlin.de

‡ To whom correspondence may be addressed at: Department of Chemistry, Syracuse University, Syracuse, NY 13244-4100, USA.

© 1998 American Society for Photobiology 0031-8655/98 \$5.00+0.00

§ Abbreviations: DME, dimethoxyethane; DMF, dimethylformamide; NOE, nuclear Overhauser effect; OEC, *trans*-2,3,7,8,12,13,17,18-octaethylchlorin; OEP, 2,3,7,8,12,13,17,18-octaethylporphyrin; TFA, trifluoroacetic acid; THF, tetrahydrofuran; TLC, thin-layer chromatography; TMS, trimethylsilane.

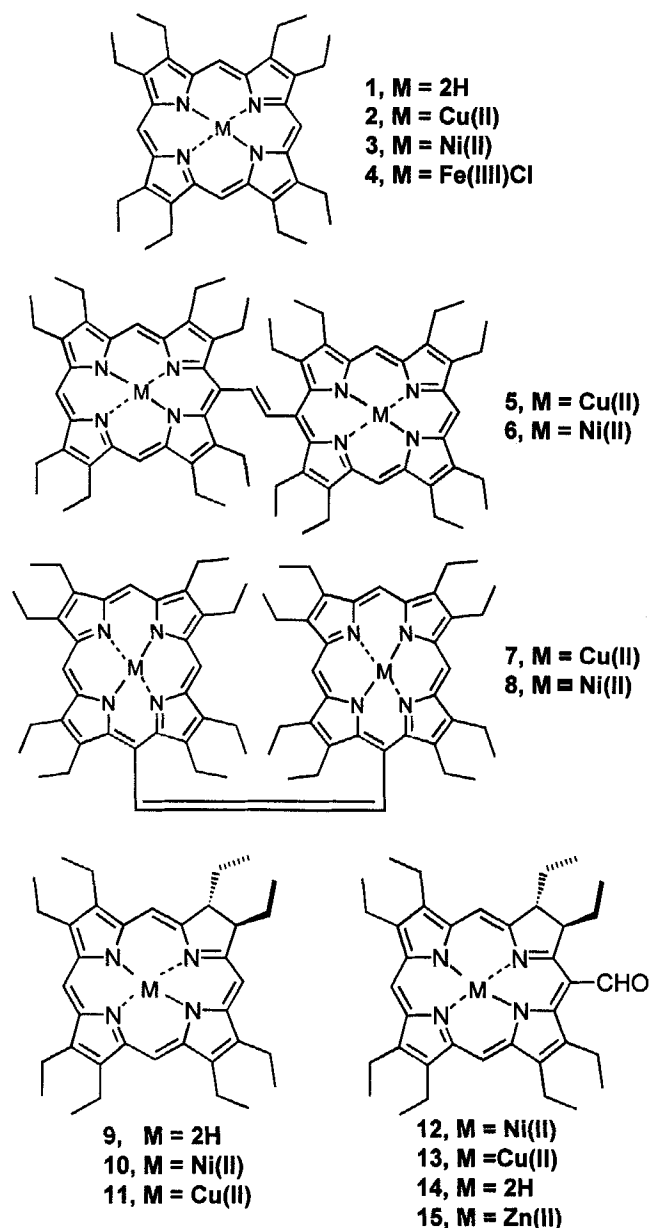


Figure 1. Chemical formulas of porphyrins 1–4, (*E*- and (*Z*)-bisporphyrins 5–8, chlorins 9–11 and formylchlorins 12–15.

er face-to-face bisporphyrins this structural feature roughly mimics the arrangement of the special pair in the reaction center. Subsequently, this method has been used for the synthesis of several bistetrapyrrole systems (23–25). In this paper, we describe our results toward the synthesis of cofacial bischlorins and present the first structural data on such systems. Part of this work has been published in a preliminary communication (26).

MATERIALS AND METHODS

General. All chemicals used were of analytical grade and were purchased from Aldrich Co. Melting points were measured on a Reichert Thermovar apparatus and are uncorrected. Silica gel 60 (Merck) or basic alumina (Alfa) (usually Brockmann grade III, *i.e.* deactivated with 7% water) was used for column chromatography. Analytical thin-layer chromatography (TLC) was carried out using

Merck silica gel 60 plates or alumina 60 (neutral, fluorescence indicator F₂₅₄) plates (precoated sheets, 0.2 mm thick). Reactions were monitored by TLC and visible spectrophotometry and carried out in dimmed light. All dimerization reactions were performed under purified argon atmosphere by using modified Schlenk techniques and dry and degassed solvents. Proton NMR spectra were recorded at a frequency of 250 MHz (AC 250) or 500 MHz (Bruker, AMX 500); ¹³C-NMR spectra are ¹H broadband decoupled and were recorded at a frequency of 125 MHz. All chemical shifts are given in ppm, referenced on the δ scale downfield from the trimethylsilane (TMS) signal as internal standard. Electronic absorption spectra were recorded on a Specord S10 (Carl Zeiss) spectrophotometer using dichloromethane as solvent. Mass spectra were recorded using a Varian MAT 711 mass spectrometer using the EI technique with direct insertion probe and excitation energy of 80 eV. Elemental analyses were performed with a Perkin-Elmer 240 analyzer.

Syntheses. The synthesis of octaethylporphyrin **1** (27), octaethylchlorin **9** (28–31) and the corresponding Ni(II) and Cu(II) complexes followed published procedures (32). Purification of **9** was achieved more conveniently *via* column chromatography on alumina (toluene/*n*-hexane) and recrystallization from dichloromethane/hexane.

Vilsmeier formylation of metallochlorins. Formylation reactions were performed using a modification of the method given by Smith *et al.* (33). A solution of 610 mg (1.02 mmol) metallochlorin (either **10** or **11**) in 125 mL 1,2-dichloroethane was added during a period of 15 min to an ice-cooled mixture of 2 mL POCl₃ and 2 mL dimethylformamide (DMF) in 5 mL 1,2-dichloroethane. After removal of the ice bath the mixture was heated to 50°C for 15 min and treated with 250 mL of a saturated solution of sodium acetate. The mixture was refluxed under vigorous stirring for 2.5 h, cooled to room temperature and diluted with 500 mL dichloromethane. The organic phase was washed with water and 5% sodium hydrogen carbonate. After drying over Na₂SO₄ the solvent was evaporated. Column chromatography on neutral alumina (grade III) with toluene and recrystallization from dichloromethane/*n*-hexane or methanol yielded the respective metalloformylchlorins (**12** or **13**) in 80% yield.

(*trans*-2,3,7,8,12,13,17,18-Octaethyl-5-formylchlorinato) nickel(II), **12**. Melting point 260°C. UV/visible (CH₂Cl₂): λ_{\max} (log ϵ) = 385sh nm (4.62), 415 (4.86), 503 (3.66), 599sh (3.83), 654 (4.38). ¹H NMR (500 MHz, CDCl₃): δ = 0.97 (t, ³J = 7.5 Hz, 3H, 2²-H), 1.08 (t, ³J = 7.5 Hz, 3H, 3²-H), 1.34, 1.46 (each m, 2H, 3¹-H), 1.64, 1.75 (each m, 2H, 2¹-H), 1.46, 1.530, 1.532, 1.55, 1.56, 1.58, 1.64 (each t, ³J = 7.5 Hz, 18H, 7²-, 8²-, 12²-, 13²-, 17²-, 18²-H), 3.19–3.51 (m, 12H, 7¹-, 8¹-, 12¹-, 13¹-, 17¹-, 18¹-H), 3.86 (t, ³J = 7 Hz, 1H, 2-H), 4.71 (dd, ³J_A = 7.3 Hz, ³J_{BX} = 3 Hz, 1H, 3-H), 7.73 (s, 20-H), 8.62, 8.69 (each s, 2H, 10-, 15-H), 11.06 (s, 1H, CHO). MS (80 eV); *m/z* (%): 620 (100) [M⁺], 310 (12) [M²⁺]. C₃₇H₄₆N₄O_{Ni} (621.50): calculated C 71.50, H 7.46, N 9.01; found C 71.54, H 7.39, N 8.86.

(*trans*-2,3,7,8,12,13,17,18-Octaethyl-5-formylchlorinato) copper(II), **13**. Melting point 210°C. UV/visible (CH₂Cl₂): λ_{\max} (log ϵ) = 388sh nm (4.79), 410 (5.01), 502 (3.71), 594 (3.89), 648 (4.45). MS (80 eV); *m/z* (%): 625 (100) [M⁺], 312 (6) [M²⁺]. C₃₇H₄₆N₄O_{Cu}·0.5CH₃OH (642.4): calculated C 70.12, H 7.53, N 8.72; found C 70.43, H 7.31, N 8.48. [C₃₇H₄₆N₄O_{Cu}]⁺: calculated 625.2968; found 625.2944 (HRMS).

trans-2,3,7,8,12,13,17,18-Octaethyl-5-formylchlorin, **14**. 620 mg (1 mmol) of the nickel chlorin **12** were dissolved in 50 mL degassed concentrated sulfuric acid and gently heated up under argon for 20 min to 50°C. The reaction mixture was poured into 800 mL of a saturated solution of sodium acetate and then extracted with dichloromethane. The organic layer was washed neutral with water and dried by filtration through neutral alumina. Column chromatography on neutral alumina (grade III) with toluene/*n*-hexane followed by recrystallization from dichloromethane/*n*-hexane yielded 270 mg (0.48 mmol, 48%) of **14**. As side products 30 mg of 2,3,7,8,12,13,17,18-octaethyl-5-formylporphyrin (5%), 40 mg of **9** (7%) and 35 mg of **1** (6.5%) were obtained. Melting point 216°C. UV/visible (CH₂Cl₂ + 1% NEt₃): λ_{\max} (log ϵ) = 407 nm (5.20), 503 (3.96), 539 (3.59), 619 (3.40), 679 (4.55). UV/visible (CH₂Cl₂ + 1% TFA): λ_{\max} (log ϵ) = 412 nm (5.19), 526 (3.62), 572 (3.57), 611 (3.87), 664 (4.49). ¹H NMR (500 MHz, CDCl₃): δ = -0.69, -0.43 (s, 2-H, NH), 1.018, 1.027 (each t, ³J = 7.5 Hz, 6H, 2²-, 3²-H), 1.65,

1.66, 1.68, 1.69, 1.70, 1.71 (each t, $^3J = 7.5$ Hz, 18H, 7²⁻, 8²⁻, 12²⁻, 13²⁻, 17²⁻, 18²⁻-H), 1.49–1.62, 1.94–2.07, 2.21 (each m, 4H, 2¹⁻, 3¹⁻-H), 3.64–3.91 (m, 12H, 7¹⁻, 8¹⁻, 12¹⁻, 13¹⁻, 17¹⁻, 18¹⁻-H), 4.26, 5.11 (each m, 2H, 2⁻, 3⁻-H), 8.61, 9.34, 9.59 (each s, 3H, 10⁻, 15⁻, 20⁻-H), 11.92 (s, 1H, CHO). MS (80 eV); m/z (%): 564 (80) [M⁺], 535 (100) [M⁺-CHO], 282 (19) [M²⁺]. C₃₇H₄₈N₄O (564.81): calculated C 78.68, H 8.57, N 9.92; found C 78.46, H 8.45, N 9.50. [C₃₇H₄₈N₄O]⁺: calculated 564.3828; found 564.3857 (HRMS).

(trans-2,3,7,8,12,13,17,18-Octaethyl-5-formylchlorinato)zinc(II), **15**. Using a standard procedure the metallation of **9** was performed under argon in 90% yield (**28**). Melting point 300°C. UV/visible (CH₂Cl₂): λ_{max} (log ε) = 372sh (4.54), 395sh (4.78) 410 nm (5.03), 508 (3.61), 547 (3.58), 645 (4.34), 740 (3.86). ¹H NMR (250 MHz, d₆-DMSO): δ = 0.96, 0.98 (each t, $^3J = 7.5$ Hz, 6H, 2², 3²-H), 1.41–1.66 (m, 18H, 7²⁻, 8²⁻, 12²⁻, 13²⁻, 17²⁻, 18²⁻-H), 1.67, 1.89, 2.06 (each m, 4H, 2¹⁻, 3¹⁻-H), 3.28–3.70 (m, 12H, 7¹⁻, 8¹⁻, 12¹⁻, 13¹⁻, 17¹⁻, 18¹⁻-H), 4.10, 4.92 (each m, 2H, 2⁻, 3⁻-H), 8.27 (s, 1H, 20⁻-H), 9.04, 9.15 (each s, 2H, 10⁻, 15⁻-H), 11.61 (s, 1H, CHO). MS (80 eV); m/z (%): 626 (100) [M⁺], 313 (9) [M²⁺]. C₃₇H₄₆N₄OZn·0.5H₂COH (644.20): calculated C 69.75, H 7.43, N 8.79; found C 69.53, H 7.15, N 8.74. [C₃₇H₄₆N₄OZn]⁺: calculated 626.2963; found 626.2933 (HRMS).

McMurry coupling of **12** and **13**. Samples containing 180 mg (0.62 mmol) titanium chloride-dimethoxyethane (TiCl₃(DME)) (**17**) and 120 mg of Zn/Cu-couple were heated under reflux with 5 mL DME for 2 h. Metalloformylchlorin (50 mg, 0.08 mmol) in 10 mL DME was added to the warm reaction mixture and refluxed for 30 min. The mixture was cooled to room temperature, filtered through alumina, and the solvent removed in vacuum. The residue was then subjected to column chromatography on neutral alumina (Brockmann grade III).

Column chromatographic separation of the mixture of the coupling products of **12** on neutral alumina (Brockmann grade III) with *n*-hexane containing 1.5% tetrahydrofuran (THF) yielded the following products in the order of elution: **10** NiOEC (1.5 mg, 0.0024 mmol, 3%), *meso*-(Z)-**16** (3.5 mg, 0.003 mmol, 7%), *meso*-(E)-**17** (25 mg, 0.021 mmol, 52%), and (E)-**19** (5.5 mg, 0.0044 mmol, 11%). In addition, NiOEP (**3**) (1.5 mg, 0.0024 mmol, 3%) were found. The (E)-anti-dimer *meso*-(E)-**18** (5.5 mg, 0.0044 mmol, 11%) was isolated as an insoluble green precipitate. All products were recrystallized under inert atmosphere from a mixture of dichloromethane and *n*-hexane.

Analytical TLC of the product mixture of the McMurry coupling of **13** revealed this fraction to consist of five green fractions that were all identified as bischlorins via UV/visible spectroscopy. Preparative column chromatography on neutral alumina (grade III) with *n*-hexane containing 10% dichloromethane allowed the separation of two green fractions preceded by a blue band that was identified as Cu(II)OEC (**11**) (2 mg, 0.0032 mmol, 4%). The first green fraction contained three compounds that were separated by preparative TLC on alumina plates (Merck, neutral alumina, *n*-hexane/2.5% THF). The fastest running band (2 mg, 0.0016 mmol, 4%) could not be identified conclusively but is presumed to be the intramolecular aggregated dimer *rac*-(Z)-**20** (λ_{max} in CH₂Cl₂ [rel. int.]: 394 nm [1.00], 414sh [0.89], 505 [0.34], 623 [0.47], 642 [0.40]). The second band was identified as the unaggregated dimer *rac*-(Z)-**20** (5 mg, 0.004 mmol, 10%) followed by *rac*-(E)-**21** (5 mg, 0.004 mmol, 10%). The second green fraction (15 mg) consisted of two compounds with identical absorption spectra that could not be separated via preparative TLC. Repeated TLC of this fraction on analytical plates allowed the separation of 4 mg of *meso*-(E)-**22** (0.0032 mmol, 8%).

Meso-(Z)-1,2-anti-bis[(trans-2,3,7,8,12,13,17,18-octaethylchlorinato-5-yl)nickel(II)]-ethene, *meso*-(Z)-**16**. Melting point 260°C. UV/visible (CH₂Cl₂): λ_{max} (log ε) = 411 nm (5.02), 463 (4.84), 665 (4.61). ¹H NMR (500 MHz, CDCl₃): δ = 0.13 (t, $J = 7.5$ Hz, 6H, 7²⁻, 7²-H), 0.64 (t, $J = 7.5$ Hz, 6H, 2²⁻, 2²-H), 0.81 (t, $J = 7.5$ Hz, 6H, 3²⁻, 3²-H), 0.96, 1.14 (each m, 4H, 7¹⁻, 7¹-H), 1.20 (t, $J = 7.5$ Hz, 6H, 8²⁻, 8²-H), 1.10, 1.29 (each m, 4H, 8¹⁻, 8¹-H), 1.44, 1.45, 1.68, 1.73 (each t, $J = 7.5$ Hz, 24H, 12²⁻, 12²-, 13²⁻, 13²-, 17²⁻, 17²-, 18²⁻, 18²-H), 1.64, 2.20 (each m, 4H, 3¹⁻, 3¹-H), 1.10, 2.20 (each m, 4H, 2¹⁻, 2¹-H), 3.20–3.75 (m, 16H, 12¹⁻, 12¹-, 13¹⁻, 13¹-, 17¹⁻, 17¹-, 18¹⁻, 18¹-H), 3.77 (m, 2H, 2⁻, 2⁻-H), 4.08 (m, 2H, 3⁻, 3⁻-H), 7.23 (s, 2H, 5¹⁻, 5¹-H), 7.56, 8.74 (each s, 6H, 10⁻, 10⁻-, 15⁻, 15⁻-, 20⁻, 20⁻-H). MS (80 eV); m/z (%): 1210 (65) [M⁺], 618 (40)

[(¹/₂M + CH₂)⁺], 604 (100) [M²⁺ or (¹/₂M)⁺], 590 (52) [(¹/₂M - CH₂)⁺]. C₇₄H₉₂N₈Ni₂·1.5H₂O (1238.02): calculated C 71.79, H 7.73, N 9.05; found C 71.83, H 7.46, N 8.77. [C₇₄H₉₂N₈Ni₂]⁺: calculated 1208.6152; found 1208.6147 (HRMS).

Meso-(E)-1,2-syn-bis[(trans-2,3,7,8,12,13,17,18-octaethylchlorinato-5-yl)nickel(II)]-ethene, *meso*-(E)-**17**. Melting point 217°C. UV/visible (CH₂Cl₂): λ_{max} (log ε) = 412 nm (4.95), 459 (4.86), 654 (4.63). ¹H NMR (500 MHz, CDCl₃): δ = 0.99 (t, $J = 7.5$ Hz, 6H, 2²⁻, 2²-H), 1.00 (t, $J = 7.5$ Hz, 6H, 3²⁻, 3²-H), 1.03 (t, $J = 7.5$ Hz, 6H, 7²⁻, 7²-CH₃), 1.48, 1.49, 1.58, 1.59, 1.64, (each t, $J = 7.5$ Hz, 30H, 8²⁻, 8²-, 12²⁻, 12²-, 13²⁻, 13²-, 17²⁻, 17²-, 18²⁻, 18²-H), 1.42, 1.60 (each m, 4H, 3¹⁻, 3¹-H), 1.78, (m, 4H, 2¹⁻, 2¹-H), 3.11, 3.50 (each m, 4H, 7¹⁻, 7¹-H), 3.32, 3.38–3.59 (each m, 20H, 8¹⁻, 8¹-, 12¹⁻, 12¹-, 13¹⁻, 13¹-, 17¹⁻, 17¹-, 18¹⁻, 18¹-H), 3.85 (m, 2H, 2⁻, 2⁻-H), 4.12 (m, 2H, 3⁻, 3⁻-H), 7.23 (s, 2H, 5¹⁻, 5¹-H), 7.75 (s, 2H, 20⁻, 20⁻-H), 8.76, 8.81 (each s, 4 H, 10⁻, 10⁻-, 15⁻, 15⁻-H). MS (80 eV); m/z (%): 1210 (19) [M⁺], 630 (11) [(¹/₂M + C₂H₄)⁺], 604 (89) [M²⁺ or (¹/₂M)⁺], 590 (100) [(¹/₂M - CH₂)⁺], 575 (12) [(¹/₂M - C₂H₅)⁺], 302 (8) [M⁴⁺ or ¹/₂M²⁺], 295 (11) [(¹/₂M - CH₂)²⁺]. C₇₄H₉₂N₈Ni₂ (1210.99): calculated C 77.40, H 7.66, N 9.25; found C 73.36, H 7.63, N 9.02. [C₇₄H₉₂N₈Ni₂]⁺: calculated 1208.6152; found 1208.6149 (HRMS).

Meso-(E)-anti-bis[(trans-2,3,7,8,12,13,17,18-octaethylchlorinato-5-yl)nickel(II)]-ethene, *meso*-(E)-**18**. Melting point 307–309°C. UV/visible (CH₂Cl₂): λ_{max} (log ε) = 412 nm (4.96), 464 (4.90), 661 (4.67). ¹H NMR (500 MHz, CDCl₃): δ = 0.95 (t, $J = 7.5$ Hz, 6H, 7²⁻, 7²-H), 1.02 (t, $J = 7.5$ Hz, 6H, 3²⁻, 3²-H), 1.07 (t, $J = 7.5$ Hz, 6H, 2²⁻, 2²-H), 1.44, 1.48, 1.567, 1.572, 1.62 (each t, $J = 7.5$ Hz, 30H, 8²⁻, 8²-, 12²⁻, 12²-, 13²⁻, 13²-, 17²⁻, 17²-, 18²⁻, 18²-H), 1.45, 1.69 (each m, 4H, 3¹⁻, 3¹-H), 1.85, (m, 4H, 2¹⁻, 2¹-H), 2.96, 3.20 (each m, 4H, 7¹⁻, 7¹-H), 3.29–3.36, 3.42–3.58 (each m, 20H, 8¹⁻, 8¹-, 12¹⁻, 12¹-, 13¹⁻, 13¹-, 17¹⁻, 17¹-, 18¹⁻, 18¹-H), 3.94 (m, 2H, 2⁻, 2⁻-H), 4.43 (m, 2H, 3⁻, 3⁻-H), 7.31 (s, 2H, 5¹⁻, 5¹-H), 7.80 (s, 2H, 20⁻, 20⁻-H), 8.76, 8.77 (each s, 4H, 10⁻, 10⁻-, 15⁻, 15⁻-H). MS (80 eV); m/z (%): 1210 (100) [M⁺], 618 (22) [(¹/₂M + CH₂)⁺], 604 (53) [M²⁺ or (¹/₂M)⁺], 590 (50) [(¹/₂M - CH₂)⁺], 576 (17) [(¹/₂M - C₂H₄)⁺]. C₇₄H₉₂N₈Ni₂·H₂COH (1243.04): calculated C 72.47, H 7.78, N 9.01; found C 72.60, H 7.58, N 9.10. [C₇₄H₉₂N₈Ni₂]⁺: calculated 1208.6152; found 1208.6153 (HRMS).

5-[(E)-1,2-[(2,3,7,8,12,13,17,18-octaethylporphyrinato-5-yl)nickel(II)]ethene]-[(trans-2,3,7,8,12,13,17,18-octaethylchlorinato)nickel(II)], (E)-**19**. This compound can also be prepared by gently refluxing *meso*-(E)-**17** with traces of trifluoroacetic acid (TFA). Heating of 10 mg (0.008 mmol) of **17** in 5 mL dichloromethane and one drop TFA under reflux for 12 h followed by workup as described above yielded (E)-**19** in 60% yield. Melting point >325°C. UV/visible (CH₂Cl₂): λ_{max} (log ε) = 418 nm (4.94), 470 (4.93), 552 (4.21), 655 (4.52). ¹H NMR (500 MHz, CDCl₃): δ = 0.41 (t, $J = 7.5$ Hz, 3H, 7²-H), 0.67 (t, $J = 7.5$ Hz, 3H, 2²-H), 1.07 (t, $J = 7.5$ Hz, 3H, 3²-H), 1.35 (m, 6H, 3²⁻, 7²-H), 1.43 (m, 6H, 2²⁻, 8²-H), 1.53–1.83 (m, 27H, 8²⁻, 12²⁻, 12²-, 13²⁻, 13²-, 17²⁻, 17²-, 18²⁻, 18²-H), 1.40 (m, 2H, 2¹-H), 1.69 (m, 2H, 3¹-H), 2.80, 3.09 (each m, 2H, 7¹-H), 3.20–3.95 (m, 28H, 2¹⁻, 3¹⁻, 7¹⁻, 8¹⁻, 8¹-, 12¹⁻, 12¹-, 13¹⁻, 13¹-, 17¹⁻, 17¹-, 18¹-, 18¹-H), 2⁻, 3⁻-H), 6.18 (d, $J = 15.5$ Hz, 1H, 5¹-H), 7.62 (s, 1H, 20⁻-H), 8.03 (d, $J = 15.5$ Hz, 1H, 5¹-H), 8.76, 8.84 (each s, 2H, 10⁻, 15⁻-H), 9.36 (s, 3 H, 10⁻-, 15⁻-, 20⁻-H). MS (80 eV); m/z (%): 1208 (25) [M⁺], 604 (51) [M²⁺ or (¹/₂M)⁺], 590 (100) [(¹/₂M - CH₂)⁺], 576 (22) [(¹/₂M - C₂H₄)⁺], 295 (11) [(¹/₂M - CH₂)²⁺]. [C₇₄H₉₀N₈Ni₂]⁺: calculated 1206.5995; found 1206.5988 (HRMS).

Rac-(Z)-1,2-anti-bis[(trans-2,3,7,8,12,13,17,18-octaethylchlorinato-5-yl)copper(II)]-ethene, *rac*-(Z)-**20**. Melting point >350°C. UV/visible (CH₂Cl₂): λ_{max} (log ε) = 405 nm (5.17), 460 (4.90), 507 (4.19), 634 (4.73), 657 (4.73). MS (80 eV); m/z (%): 1220 (100) [M⁺], 609 (8) [M²⁺]. [C₇₄H₉₂N₈Cu₂]⁺: calculated 1218.6037; found 1218.6033 (HRMS).

Rac-(E)-1,2-syn-bis[(trans-2,3,7,8,12,13,17,18-octaethylchlorinato-5-yl)copper(II)]-ethene, *rac*-(E)-**21**. Melting point 309°C. UV/visible (CH₂Cl₂): λ_{max} (log ε) = 405 nm (4.97), 461 (4.56), 507 (3.97), 628 (4.53), 666 (4.31). MS (80 eV); m/z (%): 1220 (100) [M⁺], 609 (54) [M²⁺], 595 (19) [(M - CH₂)²⁺]. [C₇₄H₉₂N₈Cu₂]⁺: calculated 1218.6037; found 1218.6039 (HRMS).

Meso-(E)-1,2-anti-bis[(trans-2,3,7,8,12,13,17,18-octaethylchlorinato-5-yl)copper(II)]-ethene, *meso*-(E)-**22**. Melting point 291°C.

UV/visible (CH₂Cl₂): λ_{\max} (log ϵ) = 407 nm (5.10), 458 (4.87), 506 (4.33), 626 (4.50), 655 (4.59), 683 (4.59). [C₇₄H₉₂N₈Cu₂]⁺: calculated 1218.6037; found 1218.6064 (HRMS).

(2,3,7,8,12,13,17,18-Octaethyl-5,10-diformyloctaethylporphyrinato)copper(II), **23**. To a mixture of POCl₃ (28 mL, 45.4 g, 0.3 mol) and DMF (21 mL, 20 g, 0.3 mol) a solution of 200 mg (0.33 mmol) **2** in 200 mL 1,2-dichloroethane was added over the course of 30 min. The reaction mixture was heated under reflux for 3 h and then poured into 200 mL saturated sodium acetate solution. The reaction mixture was extracted with dichloromethane, washed neutral with water and dried by filtration through neutral aluminum oxide. Column chromatography on silica gel, eluting with dichloromethane/*n*-hexane, yielded 70 mg (0.11 mmol, 34%) (2,3,7,8,12,13,17,18-octaethyl-5-formylporphyrinato)copper **13** and 60 mg (0.09 mmol, 28%) of **23**. The product **23** was recrystallized from dichloromethane/hexane. Melting point >270°C. UV/visible (CH₂Cl₂): λ_{\max} (log ϵ) = 410 nm (5.11), 430sh (4.95), 538 (3.84), 576 (3.96), 644 (3.88). MS (80 eV); *m/z* (%): 651 (100) [M⁺], 623 (34) [M⁺ - C₂H₄], 326 (7) [M²⁺]. C₃₈H₄₄N₄O₂Cu·0.5CH₃OH (668.4): calculated C 69.19, H 6.94, N 8.38; found C 68.94, H 6.82, N 7.95.

(trans-2,3,7,8,12,13,17,18-Octaethyl-5,10-diformyloctaethylporphyrinato)copper(II), **24**. Using the general method for McMurry coupling described above, 180 mg (0.62 mmol) TiCl₃ (DME) complex (**17**) and 120 mg of Zn/Cu-couple were heated to reflux. Then, 50 mg (0.076 mmol) (2,3,7,8,12,13,17,18-octaethyl-5,10-diformylporphyrinato)copper(II) **23** in 100 mL DME was added at once and refluxed for an additional 1.5 h. After filtration through neutral alumina and removal of the solvent the residue was chromatographed on alumina eluting with *n*-hexane/dichloromethane (1:1, vol/vol). Recrystallization from dichloromethane/methanol yielded 12 mg (0.018 mmol, 24 %) blue crystals of **24**. Melting point 226°C. UV/visible (CH₂Cl₂): λ_{\max} (log ϵ) = 389 nm (4.96), 418 (4.89), 506 (3.76), 618sh (4.01), 674 (4.57). MS (80 eV); *m/z* (%): 653 (100) [M⁺], 327 (7) [M²⁺]. C₃₈H₄₆N₄O₂Cu·3CH₃OH (750.5): calculated C 65.62, H 7.79, N 7.47; found C 65.59, H 7.36, N 7.05. [C₃₈H₄₆N₄O₂Cu]⁺: calculated 653.2917; found 653.2917 (HRMS).

Crystallography. Suitable single crystals of the listed compounds were obtained by slow diffusion of a concentrated solution of the chlorins in methylene chloride into methanol (*meso*-(*Z*)-**16**, (*E*)-**19**, **24**) or ethanol (*meso*-(*E*)-**17**, *rac*-(*Z*)-**20**, *rac*-(*E*)-**21**). The crystals were immersed in hydrocarbon oil (Paraton N[®]), a single crystal selected, mounted on a glass fiber and placed in the low-temperature N₂ stream (34). Intensity data for most compounds were collected at 128 K using a Siemens P4 diffractometer with graphite monochromator and equipped with a low-temperature device. Copper K α radiation ($\lambda = 1.54178$ Å) was used for data collection that was performed with $2\theta - \theta$ scans. Cell parameters were determined from 20 to 30 reflections in the range $20^\circ \leq \theta \leq 30^\circ$. Two standard reflections were measured every 198 reflections and showed only statistical variation in intensity during data collection (<2% intensity change). The intensities were corrected for Lorentz, polarization and absorption effects (XABS2) (35); extinction effects were disregarded. The data set for (*E*)-**19** was collected using a Siemens SMART system complete with a three-circle goniometer and a charge-coupled device detector operating at 219 K utilizing Mo K α radiation ($\lambda = 0.71073$ Å). The data collection nominally covered a hemisphere of reciprocal space, by a combination of three sets of exposures: each set had a different ϕ angle, and each exposure covered 0.3° in ω . Crystal decay was monitored by repeating the initial frames at the end of the data collection and analyzing the duplicate reflections. No decay was observed for (*E*)-**19**. An absorption correction for (*E*)-**19** was applied using the program SADABS (36). The structures were solved *via* Patterson syntheses followed by subsequent structure expansion using the SHELXTL PLUS program package (37). Refinements were carried out by full-matrix least-squares on |F²| using the same program system. Hydrogen atoms were included at calculated positions by using a riding model (C-H distance 0.96 Å). Usually, no hydrogen atoms were included for solvate molecules. All calculations were carried out on a Silicon Graphics Indy workstation. With the exception of disordered positions or solvent molecules all nonhydrogen atoms were refined with anisotropic thermal parameters.

Some of the side-chain ethyl groups in *meso*-(*Z*)-**16** showed relatively high thermal parameters. Refinement with split position did

not yield an improved model. In *meso*-(*E*)-**17** two side-chain atoms (C17B and C37B) were found to be disordered and refined utilizing two split positions of equal occupancy. In addition, the structure of *meso*-(*E*)-**17** contained one heavily disordered ethanol molecule in addition to three molecules of dichloromethane. Compound (*E*)-**19** crystallized with four dichloromethane molecules of solvation. Atoms C23A, C23B, C52A and C52B were refined by introducing split positions with equal occupancy. In compound *rac*-(*Z*)-**20** three side-chain carbon atoms were found to be disordered and refined utilizing split positions of equal occupancy (C3B, C12B, C18B). The structure also contained two heavily disordered dichloromethane molecules that were refined using split positions with total occupancies of 0.5 and 0.4, respectively. In **24** one formyl group and one ethyl side chain were disordered and refined with two split positions with refined occupancies of 0.44, 0.56 for O(1) and 0.52, 0.48 for C(122).

Crystallization of (*E*)-**19** from toluene/*n*-hexane yielded a second crystalline modification in space group P $\bar{1}$ with unit cell parameters of $a = 12.398(5)$ Å, $b = 13.988(9)$ Å, $c = 22.406(3)$ Å, $\alpha = 73.50(3)^\circ$, $\beta = 87.34(4)^\circ$, $\gamma = 68.61(4)^\circ$, $V = 3462$ Å³, $Z = 2$. Compound *meso*-(*E*)-**22** crystallized from CH₂Cl₂/EtOH in space group P $\bar{1}$ with unit cell parameters of $a = 10.486(5)$ Å, $b = 12.900(5)$ Å, $c = 13.756(4)$ Å, $\alpha = 111.50(2)^\circ$, $\beta = 96.77(2)^\circ$, $\gamma = 109.36(2)^\circ$, $V = 1572$ Å³, $Z = 1$. For both compounds the molecular structure could clearly be delineated. However, due to severe disorder in both molecules refinements converged only around $R1 = 0.17$ and no further details are given here.

Further details of the crystal data, data collection, structure solutions and refinements are listed in Table 1. Complete structural data have been deposited with the CCDC.

RESULTS AND DISCUSSION

Synthesis and spectroscopy

As starting materials we chose the Ni(II) complexes, which have the advantage of being stable metallochlorins and allow NMR spectroscopic investigations. Reduction of Fe(III)OEP(Cl) **4** with sodium/isoamylalcohol (29–31), demetallation to octaethylchlorin **9**, conversion into the corresponding nickel(II) **10** and copper(II) complexes **11** followed by Vilsmeier formylation (33) gave the respective metal(II)formylchlorins **12**, **13** in a standard reaction sequence.

First, the McMurry reaction of the nickel(II) complex **12** was studied (Fig. 2). Due to the lower symmetry of the reduced OEC units compared to OEP, the formation of a variety of different isomers is possible. Treatment of **12** with low valent titanium yielded four different products, one of which was identified as the desired bischlorin dimer *meso*-(*Z*)-**16** exhibiting a (*Z*)-configuration about the connecting double bond (Fig. 3). The other two compounds were identified as different atropisomers of the respective (*E*)-ethene-linked bischlorin, distinguished by the relative orientation of the reduced pyrrole rings. In compound *meso*-(*E*)-**17**, both reduced rings were on the same side of the dimer (Fig. 4), while in *meso*-(*E*)-**18** the reduced units were on opposite sides of the molecule. This structure assignment was made upon the observation that *meso*-(*E*)-**17** could be converted into *meso*-(*E*)-**18** by treatment with traces of TFA. The (*Z*) or (*E*) orientation about the double bond and the relative arrangement of the reduced pyrrole rings was determined *via* single crystal X-ray crystallography for compounds *meso*-(*Z*)-**16**, *meso*-(*E*)-**17** and (*E*)-**19** (see below).

Small amounts of a partially oxidized bistetrapyrrole dimer were formed depending on the reaction conditions. The oxidized species was identified as the (*E*)-ethene dimer **19**, consisting of an octaethylchlorin and octaethylporphyrin moiety linked *via* an (*E*)-ethene bridge (Fig. 5). Compound

Table 1. Crystal data and refinement details for the structure determinations **16**, **17**, **19**, **20**, **21** and **24**

Chem. formula	Compound					
	<i>meso</i> -(Z)- 16	<i>meso</i> -(E)- 17	(E)- 19	<i>rac</i> -(Z)- 20	<i>rac</i> -(E)- 21	24
Mol. wt.	C ₇₄ H ₉₂ N ₈ Ni ₂ 1210.98	C ₇₄ H ₉₂ N ₈ Ni ₂ ·C ₂ H ₆ O 1511.82	C ₇₄ H ₉₀ N ₈ Ni ₂ ·2CH ₂ Cl ₂ 1378.81	C ₇₄ H ₉₂ N ₈ Cu ₂ 1305.56	C ₇₄ H ₉₂ N ₈ Cu ₂ 1220.64	C ₃₈ H ₄₆ N ₄ O ₂ Cu 654.33
Color	Black-green	Green	Blue	Green	Green	Blue-green
Habit	Plate	Block	Block	Plate	Plate	Parallelepiped
Crystal size, mm	0.24 × 0.16 × 0.01	1 × 0.58 × 0.36	0.6 × 0.4 × 0.2	0.1 × 0.01 × 0.01	0.52 × 0.35 × 0.06	0.72 × 0.26 × 0.25
Crystal system	Triclinic	Triclinic	Triclinic	Monoclinic	Monoclinic	Triclinic
Space group	P 1	P 1	P 1	P2 ₁ /c	P2 ₁ /n	P 1
<i>a</i> , Å	13.446(3)	13.960(7)	12.6082(2)	19.154(7)	19.232(7)	8.555(2)
<i>b</i> , Å	14.761(4)	16.901(10)	22.2530(2)	12.808(5)	13.085(4)	14.342(4)
<i>c</i> , Å	17.064(5)	17.252(9)	26.303(1)	28.280(11)	25.521(11)	14.775(3)
α , deg	94.67(2)	86.54(4)	106.179(1)	90	90	68.45(2)
β , deg	95.40(2)	69.48(4)	91.889(1)	98.39(3)	101.31(3)	77.76(2)
γ , deg	104.89(2)	77.00(4)	92.767(1)	90	90	80.15(2)
<i>V</i> , Å ³	3239(1)	3714(4)	7071.1(1)	6863(4)	6298(4)	1639.1(7)
<i>Z</i>	2	2	4	4	4	2
<i>D</i> _{calc} , Mg m ⁻³	1.242	1.352	1.295	1.263	1.287	1.326
μ , mm ⁻¹	1.088	3.006	0.732	1.842	1.209	1.247
Octants collected	$\pm h, \pm k, +l$	$\pm h, \pm k, +l$	$\pm h, \pm k, \pm l$	$\pm h, +k, +l$	$\pm h, +k, +l$	$\pm h, \pm k, +l$
θ _{max}	56.06	56.05	28.26	51.12	56.14	57.03
Ind. reflections	8467	9128	30 651	7376	8202	4438
Obs. reflections	6620	8828	24 707	4034	5949	3983
<i>a</i> , <i>b</i> *	0.0786, 7.0732	0.1544, 15.8571	0.0469, 12.7077	0.1096, 36.4879	0.1976, 4.3956	0.1128, 3.7079
Parameters	759	847	1617	559	757	426
Δ/σ _{max}	0.012	0.008	0.002	0.005	0.001	0.001
$\Delta\rho$ _{max} , e, Å ⁻³	1.163	1.250	1.264	0.764	1.260	1.271
R1 (I > 2.0 σ [I])	0.0610	0.0963	0.0525	0.0958	0.0898	0.0634
wR2 (I > 2.0 σ [I])	0.1470	0.2572	0.1229	0.2125	0.2368	0.1668
R1 (all data)*	0.0810	0.1070	0.0702	0.1779	0.1161	0.0693
wR2 (all data)*	0.1627	0.2735	0.1342	0.2782	0.2770	0.1735
S	1.017	1.046	1.031	1.033	1.025	1.031

*R1 = $\Sigma||F_o - F_c||/\Sigma|F_o|$, wR2 = $\{\Sigma[w(F_o^2 - F_c^2)^2]/\Sigma(w(F_o^2)^2)\}^{1/2}$, w⁻¹ = $\sigma^2(F_o^2) + (aP)^2 + bP$.

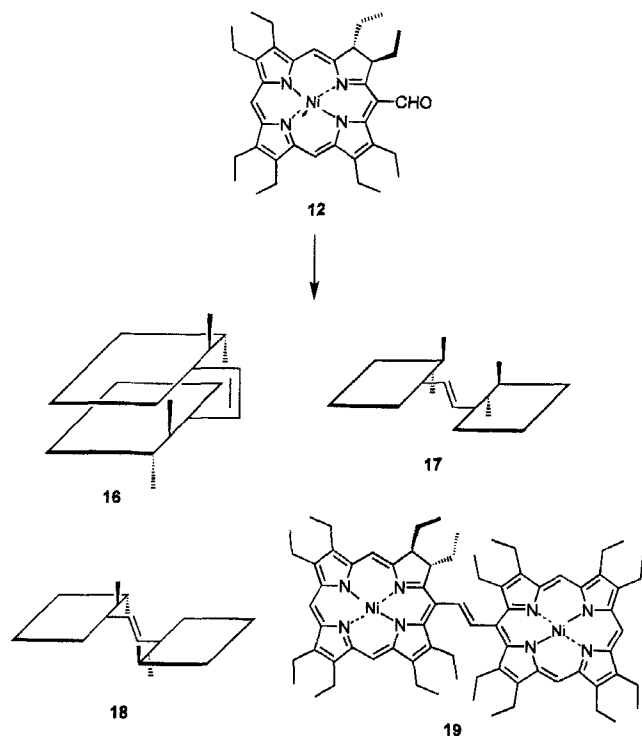


Figure 2. Chemical formulas of the reactions products **16–19** formed by McMurry coupling of **12**.

(*E*)-**19** could also be prepared directly by treatment of *meso*-(*Z*)-**16** with trace amounts of TFA in refluxing dichloromethane under air in 60% yield. Similar observations on the formation of partially oxidized bistetrapyrroles have been made by Smith and coworkers (23) during their study on the McMurry coupling of phytychlorins and rhodochlorins.

The UV/visible spectra of the various dimers are in accord with related bisporphyrin systems. Compound *meso*-(*Z*)-**16** (Soret band at 411 nm) displayed a spectrum with small hypsochromic shift as compared to that of *meso*-(*E*)-**17** (412 nm) or *meso*-(*E*)-**18** (412 nm). On the other hand, the half-oxidized dimer (*E*)-**19** exhibited a Soret band at 418 nm, *i.e.* bathochromically shifted as compared to NiOEP (391 nm), NiOEC (397 nm) or to the (*E*)-ethene porphyrin dimer **6** (414 nm) (15). On the basis of these data the configuration about the connecting double bond in **19** was assigned to be (*E*), which was confirmed by NMR spectroscopy.

The assignment of the NMR data given in the experimental section was confirmed by (*H,H*)-correlated NMR spectroscopy and nuclear Overhauser effect (NOE) experiments. The two-dimensional spectra gave detailed information for the resonance signals of both the methyl groups from the reduced pyrrole ring and the methyl group (C-72) next to the ethene bridge. Thus, it was possible to locate the signals of the methylene groups of the reduced unit, which were overlaid by other signals in the one-dimensional spectra. As an example the $^1\text{H}, ^1\text{H}$ correlated spectroscopy spectrum of *meso*-(*E*)-**17** is shown in Fig. 6. The bridge protons (51, 51') gave a NOE to the pyrrole protons H-3, while the *meso*-proton at C-20 gave a definite NOE to the pyrrole proton at C-2.

In order to study the influence of different central metals

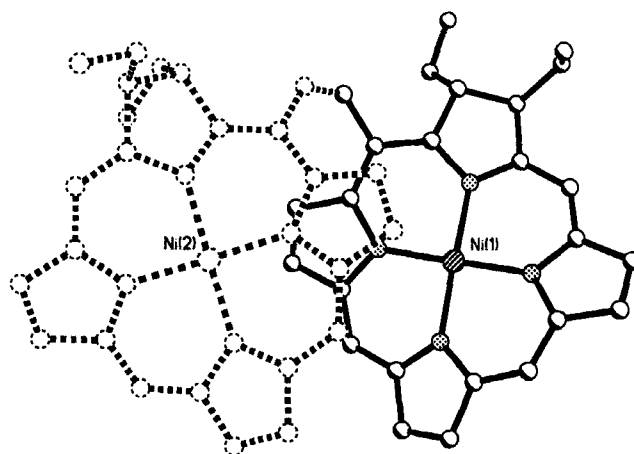
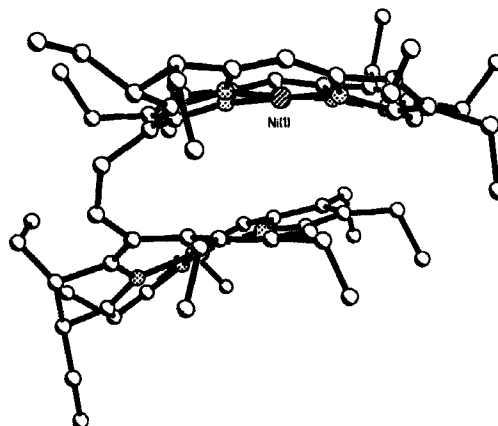


Figure 3. Side view (top) and top view (bottom) of the molecular structure of *meso*-(*Z*)-**16** in the crystal. The top view shows the molecule with the 4N plane of ring 2 [Ni(2)] in the plane of the paper. Hydrogen atoms, disordered positions and some side-chain ethyl groups have been omitted for clarity.

on the reaction and aggregation properties, we subjected the copper complex **13** to the McMurry reaction. Five green fractions, presumably all bischlorins, were identified by analytical TLC, three of which were characterized by X-ray crystallography. While compound *rac*-(*Z*)-**20** was identified

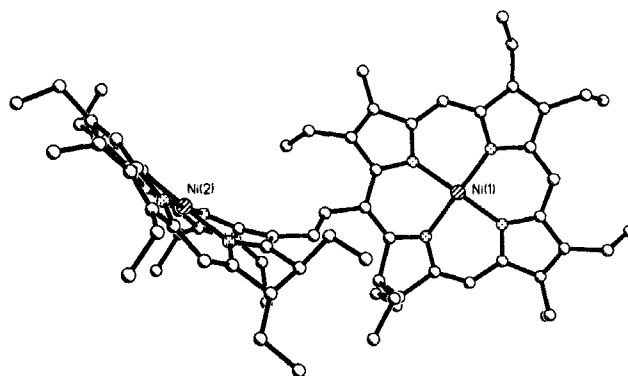


Figure 4. View of the molecular structure of *meso*-(*E*)-**17** in the crystal. Hydrogen atoms have been omitted for clarity. The molecule has been oriented so that the 4N plane of chlorin 1 (Ni1) is the plane of the paper.

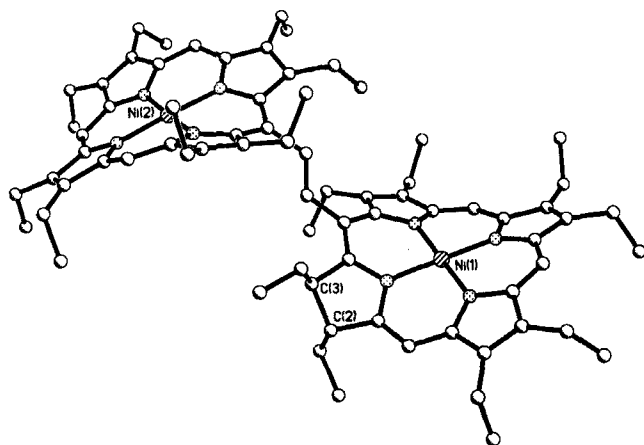


Figure 5. View of the molecular structure of (*E*)-**19** in the crystal. Hydrogen atoms have been omitted for clarity.

as an unaggregated (*Z*)-bischlorin (λ_{\max} 405 nm, Fig. 8), we observed a less polar fraction with a UV/visible spectrum showing the expected hypsochromic shift for an intramolecular aggregated arrangement of the macrocycles (λ_{\max} = 394 nm). In accordance with this result, conversion of that fraction into *rac*-(*Z*)-**20** or *rac*-(*E*)-**21** was observed during the handling of the compound. Thus the intramolecular aggregated chlorin is able to convert to the nonaggregated form

(*e.g.* *rac*-(*Z*)-**20** as shown in Fig. 8) and the (*E*)-ethene bischlorins (*e.g.* *rac*-(*E*)-**21**). Repeated attempts to crystallize the intramolecular aggregated Cu(II) bischlorin failed; consequently, an unambiguous assignment cannot be given without crystallographic data. The two other characterized fractions were identified as the *syn*-(*E*)-dimer **21** and the *anti*-(*E*)-dimer **22**, mainly differentiated by being different atropisomers. Due to the small amounts formed during the reaction, the fifth fraction could not be purified completely. On the basis of the UV/visible data, which showed spectra similar to those of *meso*-(*E*)-**22**, we suggest this compound to be a third (*E*)-ethene-linked bischlorin, presumably with a tilted macrocycle arrangement as identified in the crystal structure of *meso*-(*E*)-**17**.

Our attempts to utilize zinc(II)OEC derivatives like **15** as starting materials for the McMurry coupling failed. While Zn(II)phytychlorins and Zn(II)rhodochlorin derivatives undergo the coupling quite readily (23), compound **15** seems to be less reactive than the corresponding nickel or copper complexes **12**, **13**. Thus, longer reaction times were necessary and, despite the addition of bases like pyridine, deformation of the starting material was observed in all reactions.

The (*Z*)-ethene-bridged bischlorins and bisporphyrins easily undergo (*Z*)-(*E*) isomerization reactions, *e.g.* upon treatment with acid. In order to gain access to more stable (*Z*)-ethene-linked bistetrapyrroles, we attempted the synthesis of

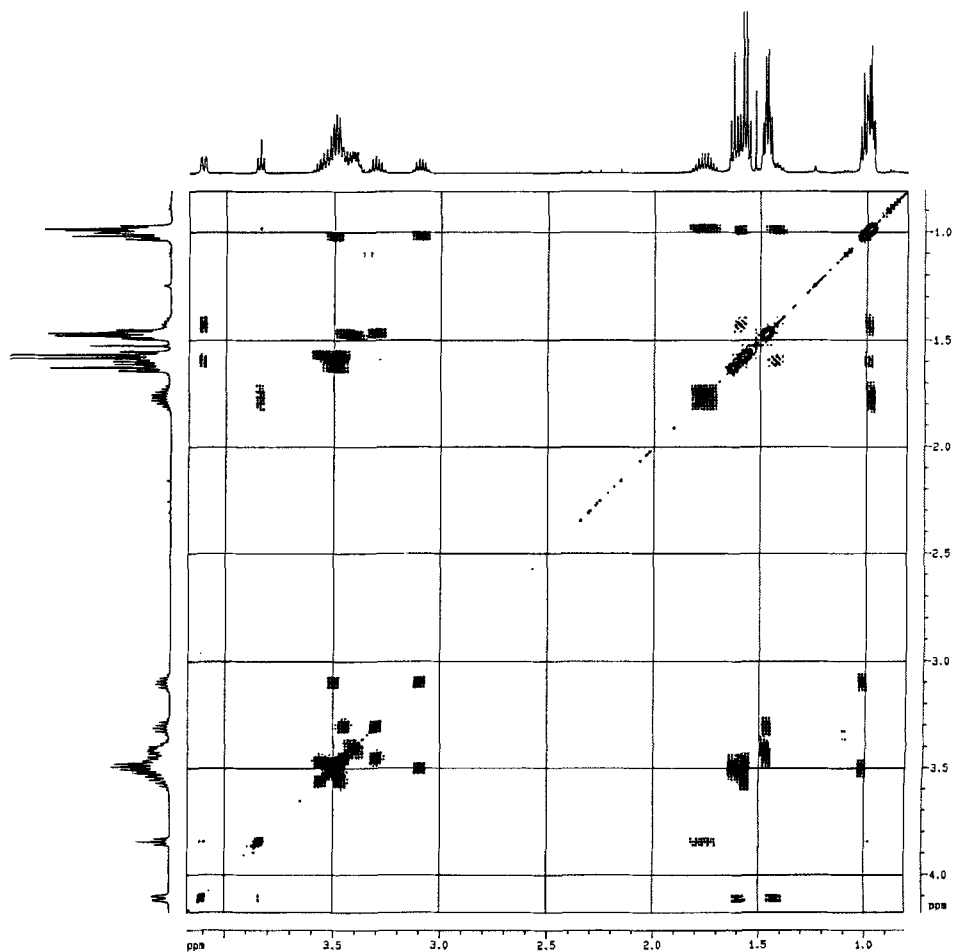


Figure 6. The $^1\text{H},^1\text{H}$ -correlated NMR spectra of the chlorin dimer **17** in CDCl_3 .

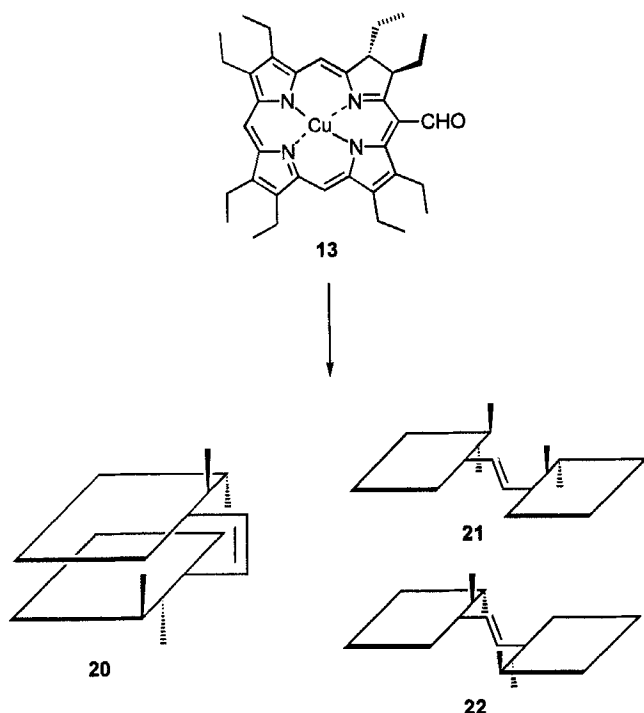


Figure 7. Chemical formulas of the reactions products 20–22 formed by McMurry coupling of 13.

bisporphyrin systems containing two connecting ethene bridges that should not undergo isomerization reactions. Suitable starting materials for such systems would be bisformyl porphyrins like Cu(II)diformyl-OEP **23**, prepared by Vilsmeier formylation of Cu(II)OEP (**2**) using excess Vilsmeier reagent and drastic reaction conditions. In our hands this reaction yielded the 5,10-diformyl derivative **23** and not Cu(II)5,15-diformyl-OEP as described in the literature (38). However, when **23** was subjected to the usual McMurry coupling reaction, bis-ethene-linked dimers were not observed;

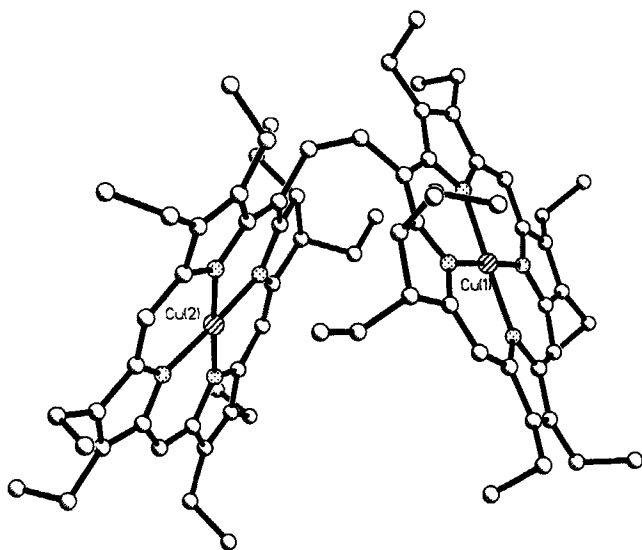


Figure 8. Side view of the molecular structure of *rac*-(*Z*)-**20** in the crystal. Hydrogen atoms and disordered positions have been omitted for clarity.

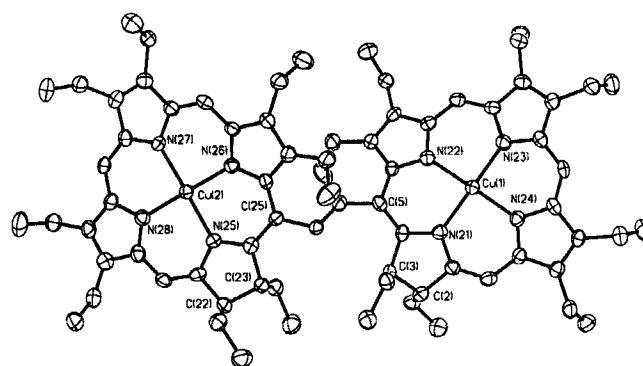


Figure 9. View of the molecular structure of *rac*-(*E*)-**21** in the crystal. Hydrogen atoms have been omitted for clarity; ellipsoids are indication for 50% occupancy.

instead, the diformylporphyrin **23** was reduced to the corresponding Cu(II)*trans*-5,20-diformyl-2,3,7,8,12,13,17,18-octaethylchlorin **24**. This compound is also accessible in low yields *via* direct formylation of Cu(II)OEP (**11**) (33). The structure of the product was unambiguously proven by a single crystal X-ray structure determination (Fig. 11).

Structural description. The crystal structures not only give information about the overall structure of the target compounds and show the differences between the (*Z*) and (*E*) forms but also show that considerable structural flexibility exists in the bischlorins. Relevant data for all dimeric aggregates are compiled in Table 2. The most notable feature is the cofacial structure with parallel macrocycle arrangement observed for *meso*-(*Z*)-**16** (Fig. 3), showing again that intramolecular aggregation stabilizes the dimers into an arrangement akin to that found in the photosynthetic reaction center. Such dimeric aggregates are best described by following the structural analysis proposed by Scheidt and Lee (16). The Ni(II)bischlorin *meso*-(*Z*)-**16** shows a much wider aggregate structure than the related Ni(II)bisporphyrin **8** (17). Thus the center-to-center separation has increased from 5.15 Å in the bisporphyrin **8** to 6.18 Å in the bischlorin *meso*-(*Z*)-**16**, while the interplanar separation has increased from 3.5 to 3.9 Å. However, the fact that effective π - π interaction in the bischlorin occurs only between two pyrrole units makes these compounds much more closely related to the naturally occurring system than the more strongly aggregated cofacial bisporphyrins. For comparison, the interplanar separation in the special pair of the photosynthetic

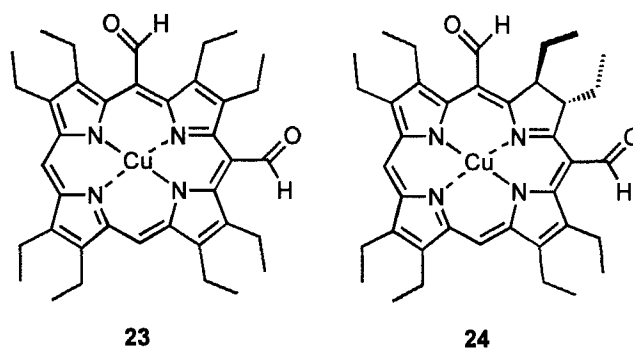


Figure 10. Chemical formulas of Cu(II)5,10-diformyl-OEP **23** and the reduction product **24**.

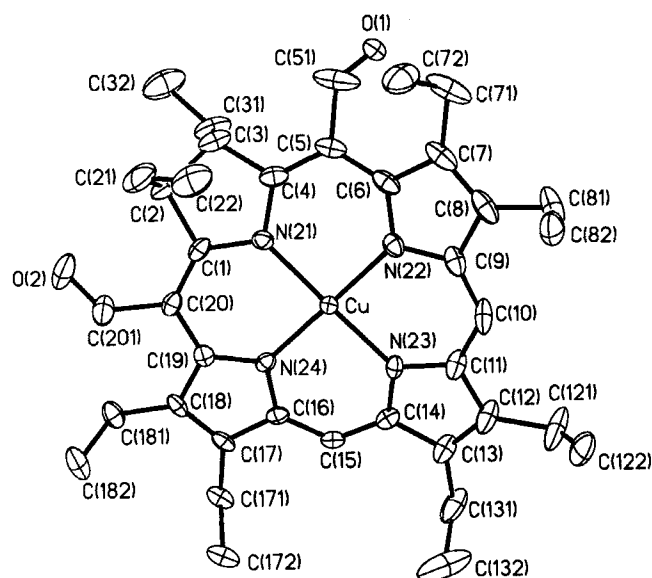


Figure 11. View of the molecular structure of **24** in the crystal. Hydrogen atoms and disordered positions have been omitted for clarity; ellipsoids indication for 50% occupancy.

reaction center varies from 3.3 to 3.8 Å while the lateral shift of the centers is in the range of 6.6–6.7 Å (1,2). Most compounds discussed here formed not only intramolecular but also intermolecular aggregates that sometimes were even stronger than the intramolecular ones. For example, compound *meso*-(*Z*)-**16** exhibits similar interplanar separations for both the intra- and intermolecular aggregates; however, the intermolecular aggregate shows a much smaller lateral shift of the metal centers. Relevant structural data for all aggregates and a comparison with the natural special pair systems have been compiled in Table 3.

The more open structure in *meso*-(*Z*)-**16** is clearly due to the higher steric demand inherent in the chlorins because of the reduced pyrrole unit. Steric considerations play an important role in facilitating the McMurry reaction for the synthesis of cofacial bistetrapyrroles. While this is easily

achieved for bisoctaethylporphyrins like **7** or **8** (17) or as shown here for bisoctaethylchlorins (albeit in much lower yield), the reaction failed to give any (*Z*) products when formylphytychlorins or rhodochlorins with propionic acid methyl ester side chains were used (33). Thus, it remains doubtful whether the McMurry coupling can be applied toward the synthesis of truly biomimetic models involving, *e.g.* bacteriopheophorbides.

An interesting observation was made with regard to the structure of the *cis*-ethene-linked Cu(II)bischlorin *rac*-(*E*)-**21** (Fig. 8). So far, all cofacial bisporphyrins for which crystal structures have been obtained show a structure in which the two macrocycles are oriented more or less parallel to each other (14,15,21,23). Thus, in all structures the arrangement observed in the solid state was one in which stabilization via intramolecular π - π aggregation had occurred (22). The present structure clearly shows that both the unaggregated and aggregated forms can be formed utilizing the McMurry reaction. The differences between the structures of *rac*-(*E*)-**21** and *meso*-(*Z*)-**16** are not due to steric constraints. Both are atropisomers with *anti*-orientation of the reduced pyrrole rings, the macrocycle conformation in *meso*-(*Z*)-**16** being more nonplanar than in *rac*-(*E*)-**21** and while both ethyl groups flanking the *meso*-bridge point outward in *rac*-(*E*)-**21**, one is pointing inward in *meso*-(*Z*)-**16**. Thus, *meso*-(*Z*)-**16** is sterically much more hindered than *rac*-(*E*)-**21**.

Intriguing variations are also observed in the structures of the (*E*)-ethene-linked bischlorins. On the basis of NMR experiments and crystal structure analyses both the Ni(II) and Cu(II) complexes of (*E*)-ethene bischlorins form an *anti*-atropisomer with an inversion center located in the $-\text{CH}=\text{CH}-$ bridge (*meso*-(*E*)-**18** for Ni on the basis of NMR and *meso*-(*E*)-**22** for Cu on the basis of a preliminary X-ray structure). This structure was expected on the basis of steric considerations and has been found previously in a variety of $-\text{CH}_2\text{CH}_2-$ -linked bistetrapyrroles as well as for **6** (17). In both series an (*E*) isomer with *syn* orientation of the reduced pyrrole units was found. In *meso*-(*E*)-**17** the two macrocycles are almost orthogonal

Table 2. Selected geometrical data for the intra- and intermolecular aggregates formed in ethene-linked bistetrapyrroles*

Compound	Aggregate type	Interplanar separation (Å)	Ct-Ct separation (Å)	Slip angle (degrees)	Lateral shift (Å)
Special pair in <i>viridis</i> (1)	<i>Rhodospseudomonas</i>	3.3	7.4	59	6.7
Special pair in <i>sphaeroides</i> (2)	<i>Rhodospseudomonas</i>	3.8	7.6	66	6.6
6 †	Intermolecular	3.922	5.756	47.1	4.217
7 †	Intramolecular	3.358	4.661	43.9	3.232
	Intermolecular	3.48	4.914	44.9	3.469
8 †	Intramolecular	3.502	5.145	47.1	3.769
	Intermolecular	3.94	6.18	50.4	4.763
<i>meso</i> -(<i>Z</i>)- 16	Intramolecular	3.9	6.176	50.8	4.786
	Intermolecular	3.988	5.733	45.9	4.117
<i>meso</i> -(<i>E</i>)- 17	No aggregation				
(<i>E</i>)- 19	No aggregation				
<i>rac</i> -(<i>Z</i>)- 20	No aggregation				
<i>rac</i> -(<i>E</i>)- 21	Intermolecular	3.729	6.14	52.8	4.89
24	Intermolecular	3.653	6.509	55.9	5.39

*Only structures with an interplanar separation of less than 4 Å were considered as aggregates.

†Data taken from Senge *et al.* (15).

Table 3. Selected structural data for the compounds studied

	Compound						
			<i>(E)</i> -19		<i>rac</i> -(<i>Z</i>)-20	<i>rac</i> -(<i>E</i>)-21	24
	<i>meso</i> -(<i>Z</i>)-16	<i>meso</i> -(<i>E</i>)-17	Molecule 1	Molecule 2			
Bond lengths, Å							
Subunit 1							
M-N21	1.937(4)	1.895(5)	1.917(2)	1.920(2)	2.018(10)	2.016(5)	2.019(3)
M-N22	1.916(4)	1.916(5)	1.913(2)	1.928(2)	2.016(8)	1.995(5)	1.990(3)
M-N23	1.923(4)	1.910(5)	1.910(2)	1.923(2)	2.008(10)	1.998(5)	1.989(3)
M-N24	1.914(4)	1.918(6)	1.909(2)	1.925(2)	1.986(9)	1.987(5)	1.986(3)
Subunit 2							
M-N25	1.915(3)	1.901(5)	1.924(2)	1.925(2)	2.026(9)	2.025(5)	—
M-N26	1.918(4)	1.925(5)	1.924(2)	1.920(2)	2.003(8)	2.019(5)	—
M-N27	1.915(3)	1.913(5)	1.921(2)	1.920(2)	1.998(9)	2.004(5)	—
M-N28	1.913(3)	1.925(6)	1.914(2)	1.927(2)	2.004(8)	2.002(5)	—
Ethene bridge							
C5–C5A	1.476(6)	1.481(9)	1.467(4)	1.477(4)	1.504(14)	1.485(8)	—
C5–C25A	1.345(6)	1.338(9)	1.353(4)	1.343(4)	1.330(14)	1.313(8)	—
C25–C25A	1.468(6)	1.466(9)	1.466(4)	1.483(4)	1.475(14)	1.488(8)	—
Torsion angles, degrees							
C5–C5A–C25A–C25	–8.2	174.4	175.9	–175.9	2.8	176.7	—
C4–C5–C5A–C25A	43.3	43.3	151.2	–145.5	–59.3	3.8	—
C6–C5–C5A–C25A	–141.3	–141.3	–30.9	34.9	122.0	–173.8	—
C5A–C25A–C25–C24	–151.7	–151.7	–137.4	127.2	–58.9	139.6	—
C5A–C25A–C25–C24	28.1	28.1	38.2	–48.6	126.3	–37.3	—
Center-to-center separation, Å							
	6.151	10.115	9.968	10.03	7.278	10.386	—
Interplanar angle, degrees							
Subunit 1/subunit 2*	22.4	87.2	11.1	10.8	132.0	13.1	0.328
Displacements, Å							
Δ24† subunit 1	0.327	0.358	0.371	0.336	0.092	0.236	0.328
Δ24† subunit 2	0.348	0.354	0.321	0.32	0.142	0.16	—

*Angle between the two 4N planes.

†Deviation of the 24 macrocycle atoms from the least-squares plane for the four nitrogen atoms.

to each other (angle between 4N planes = 87.2°) (Fig. 4), while in *rac*-(*E*)-21 the two macrocycles are almost coplanar to each other (angle between 4N planes = 13.1°) and show rotation of the ethene bridge into the macrocycle plane (Fig. 9).

The Ni–N and Cu–N bond lengths (Table 2) agree well with those described for porphyrins (16) or related Cu(II) (39) and Ni(II)chlorins (40). One notable difference to other compounds is that the difference between the M–N bond lengths for the pyrrole (N_p) and pyrroline quadrants (N_{red}) bond lengths are not as pronounced in some compounds. Typically, the M–N bond lengths involving the reduced pyrrole unit are longer than the M–N_p bonds. In subunit 1 of compound *meso*-(*E*)-17 the M–N_{red} bond is actually the shortest of all four M–N bonds. Individual bond lengths and angles are typical for those observed in porphyrins and chlorins (16).

It should be noted, that some differences are observed for the bond lengths of the connecting CH=CH bond. For most dimers C5A–C25A bond lengths typical for normal double bonds are observed (Table 3). A slightly shortened bond length of 1.313(8) Å was found in *rac*-(*E*)-21, an (*E*)-bridged Cu(II)bischlorin in which the connecting bridge is rotated into the plane between the two chlorin subunits and allows now for potential overlap of the *p*-orbitals. This arrangement has been proposed recently to account for two different spectral forms observed for the free base of 4. One spectral form

was assumed to be similar to a centrosymmetric structure like that observed for *meso*-(*E*)-22, while the other was attributed to have some degree of through-bridge conjugation of the macrocycles. In any case, the observation of different atropisomers with various degrees of macrocycle tilt relative to each other and with different conformations about the connecting double bond clearly indicates the structural flexibility inherent in these bistetrapyrrole systems.

The conformation of the individual chlorin or porphyrin macrocycles is characterized by various degrees of ruffling, *i.e.* significant out-of-plane displacement of the C_m carbon atoms induced by the metal ions (16). Overall, the degree of distortion, as indicated by the average deviation of the 24 macrocycle atoms from their least-squares plane (Δ24 in Table 2), is similar for all Ni(II)complexes, which are significantly more nonplanar than their Cu(II) counterparts. Larger differences in conformation are observed between the Cu (*Z*)/(*E*) compounds (*rac*-(*Z*)-20, *rac*-(*E*)-21) than are between *meso*-(*E*)-17 and *meso*-(*Z*)-16. As noted before (15,21), the presence of the bridging *meso*-substituents has a conformational effect and leads to significantly higher displacements of the substituted C_m positions as compared to the C_m–H groups (18% increase in displacement from the 4N plane in *meso*-(*E*)-17 to 50% in *rac*-(*E*)-21). The two formyl groups in 24 resulted in a 16% larger displacement of the substituted positions. Chlorins are generally considered to have a higher conformational flexibility than por-

phyrins. In agreement with this, the effect of the *meso* substituent is more pronounced in the porphyrin half of (*E*)-19, where an increase of 53% is observed for the substituted $C_m\text{-CH=CH-R}$ compared to $C_m\text{-H}$. The chlorin subunits show only an increase in C_m displacement by 32%. Nevertheless, the overall degree of distortion is more pronounced in the chlorin subunits, indicating that partial redistribution of the steric strain occurs.

Acknowledgements—Financial support for this project from the Deutsche Forschungsgemeinschaft (Se543/2-4 and Heisenberg stipend Se543/3-1), the Fonds der Chemischen Industrie (M.O.S.), the National Science Foundation (CHE-97-02246 and CHE-95-27898, K.R.S.) and the W. M. Keck Foundation is gratefully acknowledged.

REFERENCES

- Deisenhofer, J., O. Epp, K. Miki, R. Huber and H. Michel (1985) Structure of the protein subunit in the photosynthetic reaction centre of *Rhodospseudomonas viridis* at 3 Å resolution. *Nature* **318**, 618–624.
- Stowell, M. H. B., T. M. McPhillips, D. C. Rees, S. M. Soltis, E. Abresch and G. Feher (1997) Light-induced structural changes in photosynthetic reaction center: implications for mechanism of electron-proton transfer. *Science* **276**, 812–816.
- Wasielewski, M. R. (1993) Modeling primary electron transfer in photosynthesis using supramolecular structures. In *The Photosynthetic Reaction Center*, Vol. II (Edited by D. Deisenhofer and J. R. Norris), pp. 465–511. Academic Press, New York.
- Gust, D. and T. A. Moore (1991) Photosynthetic model systems. *Top. Curr. Chem.* **159**, 103–151.
- Wasielewski, M. R. (1992) Photoinduced electron transfer in supramolecular systems for artificial photosynthesis. *Chem. Rev.* **92**, 435–461.
- Kurreck, H. and M. Huber (1995) Model reactions for photosynthesis—photoinduced charge and energy transfer between covalently linked porphyrin and quinone units. *Angew. Chem. Int. Ed. Engl.* **34**, 849–866.
- Collman, J. P., C. M. Elliott, T. R. Halbert and B. S. Tsvog (1977) Synthesis and characterization of face-to-face porphyrins. *Proc. Natl. Acad. Sci. USA* **74**, 18–22.
- Osuka, A., S. Nakajima, K. Maruyama, N. Mataga, T. Asahi, I. Yamazaki, Y. Nishimura, T. Ohno and K. Nozaki (1993) 1,2-Phenylene-bridged diporphyrin linked with porphyrin monomer and pyromellitimide as a model for a photosynthetic reaction center: synthesis and photoinduced charge separation. *J. Am. Chem. Soc.* **115**, 4577–4589.
- Collman, J. P., D. A. Tyvoll, L. L. Chang and H. T. Fish (1995) Facile synthesis of *meso*-tetraaryl cofacial diporphyrins. *J. Org. Chem.* **60**, 1926–1931.
- Osuka, A., S. Nakajima, T. Okada, S. Taniguchi, K. Nozaki, T. Ohno, I. Yamazaki, Y. Nishimura and N. Magata (1996) Sequential electron transfer relay in diporphyrin-porphyrin-pyromellitimide triads analogous to that in the photosynthetic reaction center. *Angew. Chem. Int. Ed. Engl.* **35**, 92–95.
- Drain, C. M., R. Fischer, E. G. Nolen and J.-M. Lehn (1993) Self-assembly of a bisporphyrin supramolecular cage induced by molecular recognition between complementary hydrogen bonding sites. *J. Chem. Soc. Chem. Commun.*, pp. 243–245.
- Wasielewski, M. R., W. A. Svec and B. T. Cope (1978) Bis(chlorophyll) cyclophanes. New models of special pair chlorophyll. *J. Am. Chem. Soc.* **100**, 1961–1962.
- Senge, M. O., H. Hope and K. M. Smith (1993) Structure and conformation of photosynthetic pigments and related compounds. 6. The first crystal structure of a covalently-linked chlorin dimer—20,20'-ethylene-bis(2,3,7,8,12,13,17,18-*trans*-octaethylchlorin). *J. Chem. Soc. Perkin Trans. 2*, pp. 11–16.
- Hatada, M. H., A. Tulinsky and C. K. Chang (1980) Crystal and molecular structure of a cofacial dicopper hexyldiporphyrin-7. *J. Am. Chem. Soc.* **102**, 7115–7116.
- Senge, M. O., M. G. H. Vicente, K. R. Gerzevske, T. P. Forsyth and K. M. Smith (1994) Models for the photosynthetic reaction center—preparation, spectroscopy, crystal and molecular structures of cofacial bisporphyrins linked by *cis*-1,2- and *trans*-1,2-ethene bridges, and of 1,1-carbinol bridged bisporphyrins. *Inorg. Chem.* **33**, 5625–5638.
- Scheidt, W. R. and Y. J. Lee (1987) Recent advances in the stereochemistry of metallotetrapyrroles. *Struct. Bonding (Berlin)* **64**, 1–70.
- McMurry, J. E., T. Lectka and J. G. Rico (1989) An optimized procedure for titanium-induced carbonyl coupling. *J. Org. Chem.* **54**, 3748–3751.
- Fürstner, A. and B. Bogdanovic (1996) New developments in the chemistry of low titanium. *Angew. Chem. Int. Ed. Engl.* **35**, 2442–2469.
- Vicente, M. G. H. and K. M. Smith (1991) Vilsmeier reactions of porphyrins and chlorins with 3-(dimethylamino)acrolein to give *meso*-(2-formylvinyl)porphyrins: new syntheses of benzo-chlorins, benzoisobacteriochlorins, and benzobacteriochlorins and reductive coupling of porphyrins and chlorins using low-valent titanium complexes. *J. Org. Chem.* **56**, 4407–4418.
- Vogel, E. (1996) Porphyrinoid macrocycles: a cornucopia of novel chromophores. *Pure Appl. Chem.* **68**, 1355–1360.
- Senge, M. O., K. R. Gerzevske, M. G. H. Vicente, T. P. Forsyth and K. M. Smith (1993) Models for the photosynthetic reaction center—synthesis and structure of porphyrin dimers with *cis*-ethene and *trans*-ethene and skewed hydroxy-methylene bridges. *Angew. Chem. Int. Ed. Engl.* **32**, 750–753.
- Senge, M. O., C. W. Eigenbrot, T. D. Brennan, J. Shusta, W. R. Scheidt and K. M. Smith (1993) Aggregation properties of nitro-porphyrins—comparisons between solid state and solution structures. *Inorg. Chem.* **32**, 3134–3142.
- Jaquinod, L., D. J. Nurco, C. J. Medforth, R. K. Pandey, T. P. Forsyth, M. M. Olmstead and K. M. Smith (1996) Synthesis and characterization of bis(chlorin)s from the McMurry reaction of formylchlorins. *Angew. Chem. Int. Ed. Engl.* **35**, 1013–1016.
- Jaquinod, L., M. O. Senge, R. K. Pandey, T. P. Forsyth and K. M. Smith (1996) Planar bischlorophyll derivatives with a completely conjugated π -system—model compounds for the special pair in photosynthesis. *Angew. Chem. Int. Ed. Engl.* **35**, 1840–1842.
- Paolesse, R., R. K. Pandey, T. P. Forsyth, L. Jaquinod, K. R. Gerzevske, D. J. Nurco, M. O. Senge, S. Licoccia, T. Boschi and K. M. Smith (1996) Stepwise syntheses of bisporphyrins, bischlorins, and bischorroles, and of porphyrin-chlorin and porphyrin-corrrole heterodimers. *J. Am. Chem. Soc.* **118**, 3869–3882.
- Senge, M. O., W. W. Kalisch and K. Ruhlandt-Senge (1996) Synthesis and crystal structures of cofacial bischlorins. Octaethylchlorin-based structural models for the special pair in photosynthesis. *J. Chem. Soc. Chem. Commun.*, pp. 2149–2150.
- Sessler, J. L., A. Mozaffari and M. R. Johnson (1992) 3,4-Diethylpyrrole and 2,3,7,8,12,13,17,18-octaethylporphyrin. *Org. Synth.* **70**, 68–78.
- Kevin M. Smith (1975) *Porphyrins and Metalloporphyrins*. Elsevier, Amsterdam.
- Eisner, U., A. Lichtarowicz and R. P. Linstead (1957) Chlorophyll and related compounds. Part VI. The synthesis of octaethylchlorin. *J. Am. Chem. Soc.* **79**, 733–739.
- Inhoffen, H. H., J. W. Buchler and R. Thomas (1969) Zur weiteren Kenntnis des Chlorophylls und des Hämins, XXVI (1), *cis*- and *trans*-7,8-dihydro-octaäthylporphyrin (epimere Octaethylchlorine). *Tetrahedron Lett.* **10**, 1145–1148.
- Whitlock, H. W., R. Hanauer, M. Y. Oester and B. K. Bower (1969) Diimide reduction of porphyrins. *J. Am. Chem. Soc.* **91**, 7485–7489.
- Stolzenberg, A. M. and M. T. Stershic (1987) Solution conformations of hydrophorphyrin complexes. Synthesis and properties of K- and *trans*-octaethylchlorin complexes. *Inorg. Chem.* **26**, 1970–1977.
- Smith, K. M., G. M. F. Bisset and M. J. Bushell (1980) *Meso*-methylporphyrins and -chlorins. *Bioorg. Chem.* **9**, 1–26.
- Hope, H. (1994) X-ray crystallography: a fast, first-resort analytical tool. *Prog. Inorg. Chem.* **41**, 1–19.
- Parkin, S. R., B. Moezzi and H. Hope (1995) XABS 2: an em-

- pirical absorption correction program. *J. Appl. Crystallogr.* **28**, 53–56.
36. Sheldrick, G. M. (1996) SADABS, a program for absorption correction using area detector data. Universität Göttingen.
37. Siemens Analytical Instruments Inc. (1994) *SHELXTL PLUS*, Version 5.03. Madison, WI.
38. Watanabe, E., S. Nishimura, H. Ogoshi and Z. Yoshida (1975) Orientation of electrophilic meso-substitution in metalloctaethylporphyrins. *Tetrahedron* **31**, 1385–1390.
39. Senge, M. O., K. Ruhlandt-Senge, S.-J. H. Lee and K. M. Smith (1995) On the structure and macrocycle conformation of two copper(ii) rhodochlorin derivatives and two related rhodoporphyrins. *Z. Naturforsch.* **50b**, 969–981.
40. Senge, M. O. and K. M. Smith (1994) On the conformation of the methyl ester of (20-methyl-phytyochlorinato)nickel(ii)—a bacteriochlorophyll c model compound. *Photochem. Photobiol.* **60**, 139–142.
41. Chachisvilis, M., V. S. Chirvony, A. M. Shulga, B. Källebring, S. Larsson and V. Sundström (1996) Spectral and photophysical properties of ethylene-bridged side-to-side porphyrin dimers. 1. Ground-state absorption and fluorescence study and calculation of electronic structure of *trans*-1,2-bis(*meso*-octaethylporphyrinyl)ethene. *J. Phys. Chem.* **100**, 13857–13866.